Journal of Clinical Monitoring and Computing (2019) 33:605–613
https://doi.org/10.1007/s10877-018-0207-3

ORIGINAL RESEARCH

Cerebral arterial time constant calculated from the middle and posterior cerebral arteries in healthy subjects

Agnieszka Uryga[1] · Magdalena Kasprowicz[1] · Małgorzata Burzyńska[2] · Leanne Calviello[3] · Katarzyna Kaczmarska[4,5] · Marek Czosnyka[3,5]

Received: 18 June 2018 / Accepted: 1 October 2018 / Published online: 5 October 2018

Abstract

The cerebral arterial blood volume changes (ΔC_aBV) during a single cardiac cycle can be estimated using transcranial Doppler ultrasonography (TCD) by assuming pulsatile blood inflow, constant, and pulsatile flow forward from large cerebral arteries to resistive arterioles [continuous flow forward (CFF) and pulsatile flow forward (PFF)]. In this way, two alternative methods of cerebral arterial compliance (C_a) estimation are possible. Recently, we proposed a TCD-derived index, named the time constant of the cerebral arterial bed (τ), which is a product of C_a and cerebrovascular resistance and is independent of the diameter of the insonated vessel. In this study, we aim to examine whether the τ estimated by either the CFF or the PFF model differs when calculated from the middle cerebral artery (MCA) and the posterior cerebral artery (PCA). The arterial blood pressure and TCD cerebral blood flow velocity ($CBFV_a$) in the MCA and in the PCA were non-invasively measured in 32 young, healthy volunteers (median age: 24, minimum age: 18, maximum age: 31). The τ was calculated using both the PFF and CFF models from the MCA and the PCA and compared using a non-parametric Wilcoxon signed-rank test. Results are presented as medians (25th–75th percentiles). The cerebrovascular time constant estimated in both arteries using the PFF model was shorter than when using the CFF model (ms): [64.83 (41.22–104.93) vs. 178.60 (160.40–216.70), $p < 0.001$ in the MCA, and 44.04 (17.15–81.17) vs. 183.50 (153.65–204.10), $p < 0.001$ in the PCA, respectively]. The τ obtained using the PFF model was significantly longer from the MCA than from the PCA, $p = 0.004$. No difference was found in the τ when calculated using the CFF model. Longer τ from the MCA might be related to the higher C_a of the MCA than that of the PCA. Our results demonstrate MCA-PCA differences in the τ, but only when the PFF model was applied.

Keywords Cerebral arterial blood volume changes · Cerebral arterial time constant · Cerebral arterial compliance · Transcranial Doppler ultrasonography

✉ Agnieszka Uryga
agnieszka.uryga@pwr.edu.pl

[1] Department of Biomedical Engineering, Faculty of Fundamental Problems of Technology, Wroclaw University of Science and Technology, Wybrzeze Wyspianskiego 27, 50-370 Wrocław, Poland

[2] Department of Anesthesiology and Intensive Care, Wroclaw Medical University, Wrocław, Poland

[3] Brain Physics Laboratory, Division of Neurosurgery, Department of Clinical Neurosciences, University of Cambridge, Cambridge, UK

[4] Department of Neurosurgery, Mossakowski Medical Research Centre Polish Academy of Sciences, Warsaw, Poland

[5] Institute of Electronic Systems, Faculty of Electronics and Information Technology, Warsaw University of Technology, Warsaw, Poland

1 Introduction

Regional distribution of the cerebral vascular tone [1, 2] and the time metrics of cerebral circulation can be measured using imaging techniques such as a positron emission tomography (PET) [3] and arterial spin labeling magnetic-resonance imaging (ASL-MRI) [4, 5]. However, these methods are expensive and not suitable for continuous monitoring. An alternative technique is transcranial Doppler ultrasonography (TCD), which enables the recording of cerebral blood flow velocity in the main cerebral arteries ($CBFV_a$) in real-time to access cerebrovascular functions both in healthy volunteers and in patients (e.g., in patients with severe traumatic brain injury [6] and after aneurysmal subarachnoid haemorrhage [7]). Additionally TCD allows determining the cerebral arterial blood volume changes

(ΔC_aBV). The ΔC_aBV is influenced by the difference in pulsatile intracranial arterial inflow and the flow forward through the resistive arterioles. We have recently developed two methods for evaluating ΔC_aBV during a single cardiac cycle with TCD [8, 9]. The first presumes that cerebral blood outflow can be approximated by the mean cerebral blood inflow, considering its low pulsatile character in relation to cerebral blood inflow [10]. We named it the 'continuous flow forward' (CFF) model. The second approach, termed the 'pulsatile flow forward' (PFF) model, accounts for pulsatile blood outflow and the variability of systemic vascular impedance as a result of pulsatile changes in the arterial blood pressure (ABP) waveforms [9]. The two models of ΔC_aBV estimation imply two different methods of cerebral arterial compliance (C_a) calculation. However, both return estimators of C_a that are dependent on the cross-sectional area of the insonated cerebral vessel. We recently introduced a TCD-based cerebral hemodynamic parameter, the time constant of cerebral arterial bed (τ) [11]. Conceptually, the τ describes the time needed to stabilize the cerebral blood volume after a sudden change in ABP during one cardiac cycle [11]. Theoretically, such a volume change lasts infinitely, but 95% of volume changes happen approximately in a time interval equal to $3\times\tau$. The τ is calculated as the product of the C_a and the cerebrovascular resistance (CVR) and is expressed in seconds, therefore it can be used to compare different cerebral arteries, irrespective of diameter. The τ has been previously investigated and was suggested as an early indicator of cerebral vasospasm (CV) [12], and applied to monitor cerebrovascular reactivity in vaso-occlusive disease [13]. The τ has also been used to investigate the reaction to end-tidal CO_2 changes in healthy subjects [9, 11] and in other experimental scenarios [14].

In this study, we applied both the CFF and PFF models to determine the τ from two main cerebral arteries, the middle cerebral artery (MCA) and the posterior cerebral artery (PCA) and compared those models' abilities to differentiate the characteristics of the cerebral vasculature. We hypothesized that the PFF model, which included the influence of cerebrovascular resistance and the pulsatile character of ABP, might better reflect vascular differences than would the CFF model.

2 Materials and methods

2.1 Subjects

Data from 32 young, healthy volunteers (11 males, 21 females, median age: 24, minimum age: 18, maximum age: 31) were analyzed. All participants were asked to avoid caffeine and alcohol for 12 h before the measurements were taken. The subjects were non-smokers and free of cardiovascular or neurological diseases and medications known to affect cardiovascular parameters or cerebral blood flow.

2.2 Protocol and data acquisition

The initial sections of MCA and PCA (M1 and P1, respectively) were insonated with TCD (Doppler BoxX, DWL, Compumedics Germany GmbH, Singen, Germany) through the left and right transtemporal windows to obtain the cerebral blood flow velocity ($CBFV_a$). The MCA and the PCA were identified by their depth and Doppler spectra. A 2 MHz ultrasound probe was attached to a plastic helmet and immobilized on the volunteer's head. The ABP signal was measured non-invasively using photoplethysmography (Finometer MIDI, FMS Medical Systems, Amsterdam, The Netherlands). The electrocardiogram (ECG) was registered using a three-lead surface ECG module of Finometer MIDI. The pressure cuff was placed on the middle finger, with the hand held at heart level. The end-tidal carbon dioxide ($EtCO_2$) was recorded using a capnograph (RespSense™, NONIN, Plymouth, Minnesota, U.S.A.). An anaesthetic, facemask was applied to the patient's nose and mouth and connected to a capnograph. Each of the volunteers breathed spontaneously during the recording session. There were no significant changes in $EtCO_2$. All measurements were performed while subjects were seated in the middle of the chair with their feet on the floor for at least 5 min per session.

2.3 Data analysis

Signals were sampled at a frequency of 200 Hz. All identified distortions in ABP or $CBFV_a$ signals due to the displacement of the ultrasound probe or finger cuff, incorrect gain settings, or poor temporal bone windows were removed manually; further analysis was performed utilizing the correct parts of the signals. The algorithms embedded in the Intensive Care Monitor (ICM+) system (Cambridge Enterprise Ltd., Cambridge, U.K; http://www.neurosurg.cam.ac.uk/icmplus) and custom-written program in MATLAB® (MathWorks®, Natick, MA, U.S.A.) were used to calculate the cerebral hemodynamic parameters. Mean values of the respective signals were calculated by averaging values in a 10-s time window.

2.4 Cerebral arterial blood volume changes during a single cardiac cycle

The magnitude of the pulsatile changes in C_aBV (ΔC_aBV) during a single cardiac cycle was estimated based on methodology first proposed by Avezaat and Eijndhoven [15], and then further modified and applied in our previous works [8, 9, 16]. We named it the 'CFF' model. According to this concept, the

changes in cerebral blood volume (ΔCBV) during a single cardiac cycle can be calculated as the integral between pulsatile arterial inflow (CBF_a) and venous outflow (CBF_v):

$$\Delta CBV(t) = \int_{t_0}^{t} (CBF_a(s) - CBF_v(s))ds \quad (1)$$

where t_0 and t are the respective beginning and the end of a cardiac cycle and s is the variable of integration.

We assumed that CBF_v has a low pulsatility compared with the CBF_a, thus the CBF_v may be approximated by constant flow equal to the averaged cerebral arterial inflow ($meanCBF_a$). Therefore the ΔC_aBV can be expressed as:

$$\Delta C_aBV(t)_{CFF} = \int_{t_0}^{t} \left(CBF_a(s) - meanCBF_a\right)ds \quad (2)$$

The PFF model includes the dependency of the blood outflow on the impedance of the afferent part of the vascular system, which is controlled by the vasomotor tone of the cerebral vessels and pulsatile changes in ABP. Therefore, the ΔC_aBV can be alternatively expressed using the PFF model as:

$$\Delta C_aBV(t)_{PFF} = \int_{t_0}^{t} \left(CBF_a(s) - \frac{ABP(s)}{CVR}\right)ds \quad (3)$$

where ABP is the arterial blood pressure and CVR is the cerebrovascular resistance, defined by the following formula [16]:

$$CVR = \frac{meanABP}{meanCBFV_a \times S_a}\left(\frac{mmHg}{cm^3/s}\right) \quad (4)$$

where meanABP and $meanCBFV_a$ are averaged values of the respective signals and S_a denotes the unknown cross-sectional area of the insonated vessel. For further calculation, the value of CVR was normalized (by the S_a). Therefore, CVR was expressed in (mmHg/cm/s).

Equations (2) and (3) can be redefined when taking into account the finite sampling frequency and operating under the assumption of a constant cross-sectional area of the insonated vessel (S_a), utilizing TCD-derived $CBFV_a$ [2, 17] as follows:

$$\Delta C_aBV(n)_{CFF} = S_a \sum_{i=1}^{n} [CBFV_a(i) - meanCBFV_a]\Delta t\ (cm^3) \quad (5)$$

$$\Delta C_aBV(n)_{PFF} = S_a \sum_{i=1}^{n} \left[CBFV_a(i) - \frac{ABP(i)}{CVR}\right]\Delta t\ (cm^3) \quad (6)$$

where n is the number of samples from the beginning of the cardiac cycle, Δt is the time interval between two subsequent samples, $CBFV_a(i)$ and ABP(i) are the samples of the $CBFV_a$ and ABP, respectively, and $meanCBFV_a(i)$ is the moving-average of $CBFV_a$ from the window including several previous heart evolutions (a 6-s window was applied) [14]. Note that both ΔC_aBV_{CFF} and ΔC_aBV_{PFF} were normalized for further calculation [divided by the unknown cross-sectional area: S_a (cm^2)], resulting in expression in (cm) instead of (cm^3). Example time trends of pulse changes in ABP, $CBFV_a$, ΔC_aBV_{CFF}, and ΔC_aBV_{PFF} in both the MCA and the PCA are presented in Fig. 1a, b, respectively.

2.5 Compliance of the cerebral arterial bed

The compliance of the cerebral arterial bed (C_a) was estimated as the amplitude of ΔC_aBV_{CFF} ($Amp\Delta C_aBV_{CFF}$) or the amplitude of ΔC_aBV_{PFF} ($Amp\Delta C_aBV_{PFF}$) divided by the amplitude of ABP (AmpABP) as follows [16]:

$$C_{aCFF} = \frac{Amp\Delta C_aBV_{CFF} \times S_a}{AmpABP}\left(\frac{cm^3}{mmHg}\right) \quad (7)$$

$$C_{aPFF} = \frac{Amp\Delta C_aBV_{PFF} \times S_a}{AmpABP}\left(\frac{cm^3}{mmHg}\right) \quad (8)$$

The fundamental amplitudes AmpABP and the $Amp\Delta C_aBV_{CFF}$ were determined using Fourier Transform. The $Amp\Delta C_aBV_{PFF}$ was calculated using the following formula:

$$Amp\Delta C_aBV_{PFF} = \left(AmpCBFV_a - \frac{AmpABP}{CVR}\right)\Big/ 2\pi HR \quad (9)$$

The heart rate (HR) was calculated as the frequency of the first harmonic of the ABP signal using Fourier Transform. In the PFF model, a new proposal of $Amp\Delta C_aBV_{PFF}$ calculation was introduced to diminish the time delay between signals recorded from the cerebral arteries ($CBFV_a$) and from the finger (ABP) [9]. Note, that C_{aCFF} and C_{aPFF} were normalized by the unknown S_a, resulting in expression in (cm/mmHg).

2.6 Time constant of cerebral arterial bed

The time constant of cerebral arterial bed (τ) was calculated as the product of C_a (calculated using either the CFF or the PFF model) and CVR [11, 13]:

$$\tau_{CFF} = C_{aCFF} \times CVR\ (s) \quad (10)$$

$$\tau_{PFF} = C_{aPFF} \times CVR\ (s) \quad (11)$$

Note that the τ is independent of the cross-sectional area of the S_a. The τ_{CFF} estimates the time when

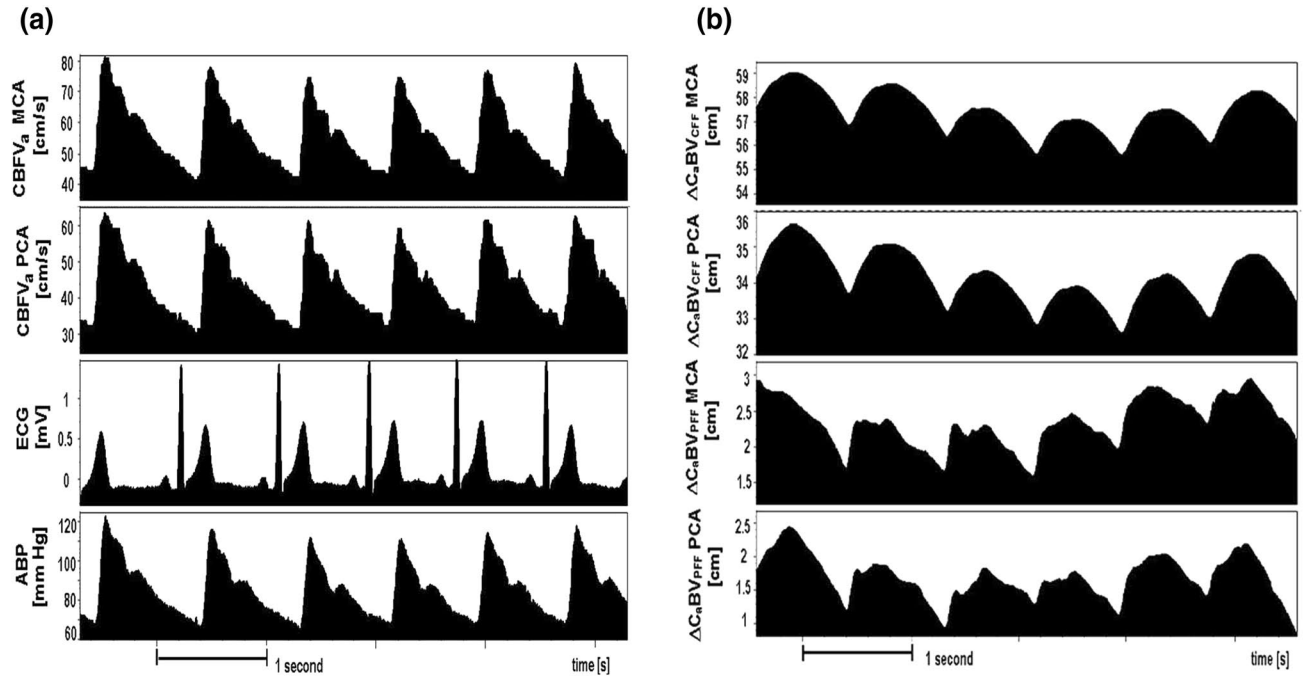

Fig. 1 **a** Time trends of systemic arterial blood pressure (ABP), electrocardiogram (ECG) and cerebral blood flow velocity ($CBFV_a$) in the middle cerebral artery (MCA) and in the posterior cerebral artery (PCA). **b** The cerebral arterial blood volume changes calculated using the pulsatile flow forward model (ΔC_aBV_{PFF}) and the continuous flow forward model (ΔC_aBV_{CFF}) in the middle cerebral artery (MCA) and in the posterior cerebral artery (PCA) in a healthy 23-year-old male volunteer

blood reaches the arterioles'/capillaries' boundary zone, whereas the τ_{PFF} reflects the time needed to fill the smaller cerebral arteries from the insonation point (Fig. 2).

2.7 Statistical analysis

Statistical analysis was conducted with STATISTICA 12 software (Statistica, StatSoft, Inc., Tulsa, Oklahoma, U.S.A). The hypothesis of normality was rejected for most of the analyzed variables based on a Shapiro–Wilk test with a Lilliefors correction. The non-parametric Wilcoxon signed-rank

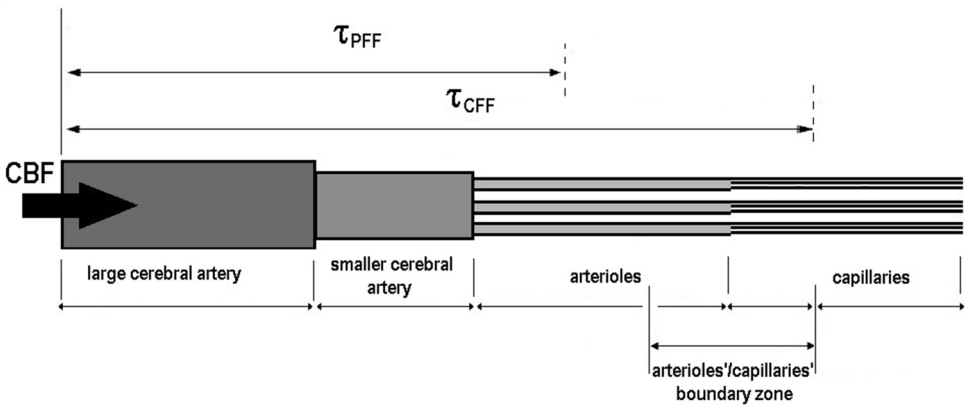

Fig. 2 The schematic structure of cerebral vasculature. Cerebral blood flow (CBF), which enters the large cerebral artery, moves forward to smaller cerebral arteries and then to distal cerebral vessels: arterioles and capillaries. The time needed to stabilize the cerebral blood volume after a sudden change in arterial blood pressure after a heart constriction (τ), calculated using the continuous flow forward model (CFF), estimates the time needed for filling the arterioles or even arterioles'/capillaries' boundary zone with blood volume, whereas the pulsatile flow forward model (PFF) describes the time to fill smaller cerebral arteries with blood volume

test was applied to evaluate the differences in physiological parameters and hemodynamic indices calculated from the MCA and the PCA using either the CFF or the PFF model. The relationship between the τ_{CFF} and τ_{PFF} was tested using a non-parametric (Spearman) correlation. The level of significance was set at 0.05. Results are presented as medians [interquartile ranges (IQR), 25th–75th percentiles].

3 Results

3.1 Physiological variables

Physiological systemic and cerebral variables in the total group of volunteers are presented in Table 1. Significantly higher values of $CBFV_a$ were found in the MCA than of those in the PCA (cm/s): 68.86 (57.01–77.11) and 34.85 (29.95–43.10); $p \ll 0.001$. Similarly, the values of the first harmonic of $CBFV_a$ ($AmpCBFV_a$) in the MCA were higher than in the PCA (cm/s): 15.52 (11.69–18.71) vs. 7.26 (5.67–8.51); $p \ll 0.001$.

3.2 Time constant of the cerebral arterial bed calculated from the MCA and the PCA using CFF and PFF models

The τ_{PFF} was shorter than the τ_{CFF} for both arteries (ms): 64.83 (41.22–104.93) vs. 178.60 (160.40–216.70), $p < 0.001$ in the MCA, and 44.04 (17.15–81.17) vs. 183.50 (153.65–204.10), $p < 0.001$ in the PCA, respectively. The τ_{PFF} from the MCA was longer than that of the PCA (ms): 64.83 (41.22–104.93) vs. 44.04 (17.15–81.17), $p = 0.004$ (Table 1). There was no statistically significant difference in the $\tau_{CFF,}$ calculated from the MCA and the PCA (ms): 178.60 (160.40–216.70) vs. 183.50 (153.65–204.10), p = n.s.,see Fig. 3. There was a moderate correlation between the τ calculated using both models (CFF and PFF) from the MCA (R Spearman = 0.62, p = 0.0002) and the PCA (R Spearman = 0.48, p = 0.008).

4 Discussion

Our results demonstrate differences in the τ calculated from the MCA and from the PCA. However, only the PFF model permits the differentiation between those two arteries.

The median values of τ_{PFF} calculated from the PCA were significantly shorter than those from the MCA. This observation may be a consequence of the variability in the average anatomical distance from either insonated artery to the resistive arterioles. The average length of the MCA M1 branch, the lateral lenticulostriate penetrating artery [18], which branches out to arterioles, varies from 38 to 40 mm [19], whereas the average length of the thalamo-perforating arteries, which branch out from the PCA P1 segment [20], ranges from 10 to 20 mm [21]. Thus, the time needed to transfer a given volume of cerebral blood from the PCA to the distal arteriolar bed might be shorter for the PCA than for the MCA. Also differences between ABP signal between the MCA and the PCA may result in differences between τ values. However, such differences in τ estimated from the MCA and the PCA were not found when the CFF model was applied. A reason for this might be that the CFF model, in contrast to the PFF model, does not include the influence of CVR and the pulsatile character of ABP. In addition, the PFF model significantly modifies the calculation of C_a [9]. The τ represents the interplay between C_a and CVR. The relationship between them is reciprocal and non-linear [14, 16]. It has been shown, in the scenario of changing end-tidal carbon dioxide concentrations, that alterations in CVR have greater impact on the τ than on C_a [11].

On the other hand, changes in ABP or cerebral perfusion pressure (CPP, the difference between ABP and intracranial pressure (ICP)) modulate the τ more so by alterations in

Table 1 Physiological systemic and cerebral parameters [the latter measured in the middle cerebral artery (MCA) or in the posterior cerebral artery (PCA)] in 32 healthy volunteers

Parameter	PCA	MCA	p-value
ABP (mmHg)	86.79 (77.21–97.71)		–
AmpABP (mmHg)	11.76 (10.21–13.98)		–
HR (beats/min)	73.61 (68.32–84.35)		–
$EtCO_2$ (mmHg)	36.86 (33.92−39.67)		–
$CBFV_a$ (cm/s)	34.85 (29.95–43.10)	68.86 (57.01–77.11)	≪0.001
$AmpCBFV_a$ (cm/s)	7.26 (5.67–8.51)	15.52 (11.69–18.71)	≪0.001
τ_{CFF} (ms)	183.50 (153.65–204.10)	178.60 (160.40–216.70)	n.s.
τ_{PFF} (ms)	44.04 (17.15–81.17)	64.83 (41.22–104.93)	0.004

Values are presented as medians [interquartile ranges (IQR), 25th–75th percentiles]

ABP arterial blood pressure, *AmpABP* amplitude (first harmonic) of ABP, *HR* heart rate, $EtCO_2$ end-tidal carbon dioxide, $CBFV_a$ cerebral blood flow velocity in the artery, $AmpCBFV_a$ amplitude (first harmonic) of $CBFV_a$, *MCA* the middle cerebral artery, *PCA* the posterior cerebral artery

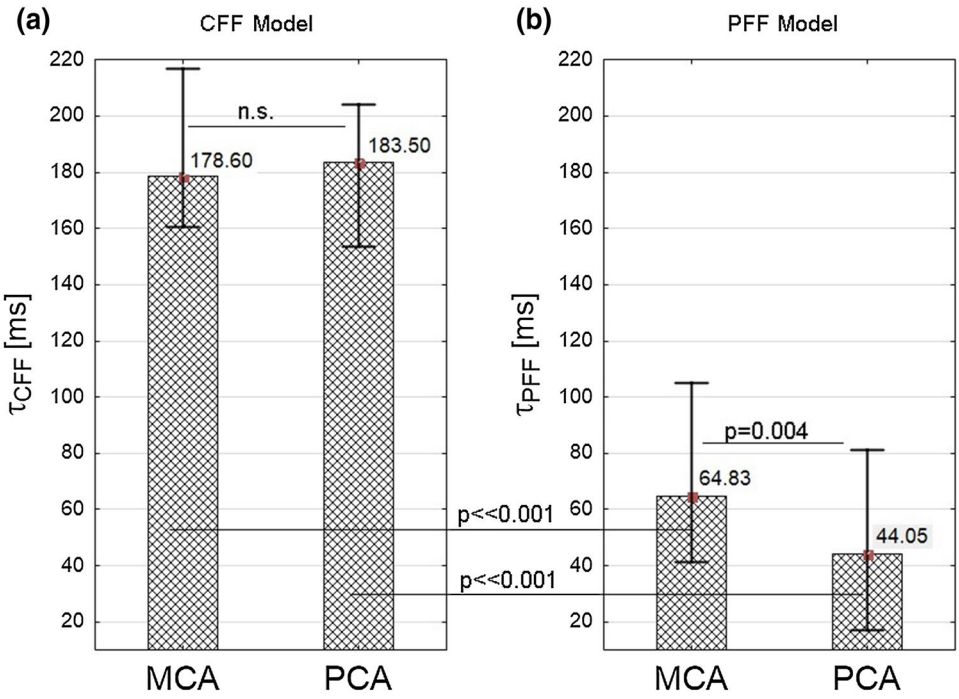

Fig. 3 The median values (boxes) and interquartile ranges (whiskers) of the time constant of the cerebral arterial bed (τ). **a** Calculated using the pulsatile flow forward model (PFF). **b** Calculated using the continuous flow forward model (CFF)

C_a and less by changes in CVR [14]. The changes in C_a are inversely correlated to changes in CPP [14]. An arterial spin-labeling magnetic resonance imaging (ASL-MRI) study has shown that in healthy normotensive subjects, the cerebral perfusion is higher in the occipital lobe (the PCA-supplied region), than in the frontal lobe (the MCA-supplied region) [22]. Since the τ represents the mutual dependency between C_a and CVR, it follows the direction of changes in C_a. Then, the shorter τ_{PFF} of PCA might be related to the lower C_a caused by the higher CPP in brain regions supplied by the PCA than by the MCA.

Results obtained for the CFF model were significantly higher than for the PFF model. The differences in the formulae of ΔC_aBV in those two models imply the differences in value of τ_{PFF} and τ_{CFF}. Since τ_{PFF} contains the influence of the pulsatile character of ABP, it may be interpreted as the time after a heart constriction when blood fills the small arteries, calculated from the insonation point. Whereas the τ_{CFF}, which assumes the constant cerebral outflow, may be the time when blood reaches the arterioles or even arterioles'/capillaries' boundary zone. Therefore, the τ_{PFF} and τ_{CFF} should be interpreted as two physiologically different cerebral blood time-related metrics: τ_{PFF}-filling time for conductive arteries only and τ_{CFF}-filling time of all compliant vascular compartments until relatively stiff dural venous sinuses (Fig. 2).

It is known, that the breathing patterns [23, 24] or the significant alterations in carbon dioxide concentration [16] may influence cerebral perfusion and cerebral hemodynamics. Hypocapnia leads to vasoconstriction and decreased cerebral blood flow and perfusion, whereas hypercapnia causes vasodilatation and increased cerebral blood flow [25, 26]. It has been shown in our previous research that hypercapnia causes a significant decrease in τ_{PFF} and τ_{CFF} from the MCA, whereas hypocapnia leads to a significant increase only in τ_{PFF} [9]. In our study, volunteers breathed spontaneously, and the $EtCO_2$ concentration was in the normocapnia range (both $EtCO_2$ and the respiratory rate (RR) were controlled during the recordings), therefore the influence of variable $EtCO_2$ was not analyzed.

In our study, we assumed that systemic ABP waveforms can be used as a surrogate of cerebral ABP waveforms, as a measurement of the latter remains a challenge. This assumption may not introduce a significant bias. The results of a modelling study performed by Zamir et al. [27] suggest that the form of the ABP wave remains unchanged as it travels from the brachial artery, where it was measured, to the MCA. There is, however, a small, constant time shift between the systemic ABP measured in the arm (or the finger in our study) and the arterial blood pressure in the cerebral vascular bed [27, 28]. Our method for $Amp\Delta C_aBV$ estimation accounts for this time shift related to the different places of measurement of the ABP and the $CBFV_a$.

In the same study Zamir et al. [27], listed different sources of cerebral compliance: intrinsic compliance of the cerebral vasculature and extravascular compliance which refers to the compliance of brain tissue and the compliance provided by changes in volume of venous blood and cerebrospinal fluid within the skull. Both our study and the study performed by Zamir et al. [27] provide non-invasive methodologies to

explore pulsatile cerebral blood flow dynamics and in particular, to explore the compliance of the cerebrovascular bed. The difference is that the approach proposed by Zamir et al. allows for the analysis of "effective compliance" which is a combination of intravascular and extravascular compliances, whereas the analysis performed in the scope of this paper focuses only on the compliance of the arterial part of the vascular bed. Although, using our methodology, an estimation of extravascular cerebral compliance is also possible, but invasive ICP signal is required as an input to the model of cerebral blood flow circulation [8, 29].

Another difference is that we used a simplified model of the cerebral blood flow circulation that consists only of two hemodynamic parameters: the C_a and the CVR, whereas the model proposed by Zamir et al. [27, 30] is more advanced and includes four properties of the vascular bed, namely: the total resistance *R*, the collective ("lumped") compliance *C* of the vessels, the viscoelastic resistance to stretch *K* within the vessel walls, and the prevailing inertial effects *L* of accelerating/decelerating flow within the vascular bed. Likely, the Zamir's model more accurately reflects pulsatile cerebral blood flow dynamics, but the simplified model used in our study is easier to interpret, thus having a greater chance to be accepted in clinical practice.

Although we were able to demonstrate in our previous study the differences in the τ between the MCA and another cerebral artery [posterior inferior cerebellar artery (PICA)], using the CFF model [31], an explanation of why differences in the τ_{CFF} were found between the MCA and PICA, but not between the MCA and the PCA, might be related to the even shorter average length of the PICA-distal vascular bed, measured from the point of insonation to small arteries, compared to the PCA branches [32, 33]. The CFF model may potentially recognize some vascular differences (e.g. the MCA vs. the PICA), but its sensitivity is not as high as that of the PFF model. Another reason may be that the CPP in the PICA-supplied region of the brain (cerebellum) is higher than the CPP in the PCA (temporal and occipital lobes). It has been shown in an imaging study [3] that another time metric of cerebral circulation, mean transient time (MTT), is inversely correlated with CPP, and is higher in the temporooccipital cortex than in the cerebellum. The MTT is a positron emission tomography (PET)-derived parameter, which refers to an average length of time when blood from an artery passes the brain tissue and is defined as the ratio between cerebral blood volume and cerebral blood flow [3, 23].

Our findings may have potential clinical applications. We have showed that in applying the PFF model, that there is a significant difference in the τ estimated from the MCA and the PCA. The results of imaging studies also showed that the MTT is longer in the temporooccipital region of the brain (MCA-supplied) and shorter in the thalamus and putamen (PCA-supplied) [1, 3]. Furthermore, an ASL-MRI study revealed that arrival arterial time (AAT), which represents the time it takes for the blood water to reach the imaging voxel, depends on the vascular territory and varies between the frontal and parietal (MCA-supplied) and temporal and occipital lobes (PCA-supplied) [4, 5, 34]. Although the MTT, the AAT, and the τ describe separate physiological concepts and vary in value, they are time-related parameters and reflect cerebral perfusion. Therefore, the τ can be applied as complementary vascular-dependent time metric of cerebral hemodynamics.

Recently, we have also demonstrated that τ_{PFF} reflects more clear reaction to changes in CO_2 concentration than does τ_{CFF} [9]. The results of other studies [35–37] suggested that the anterior and posterior parts of the brain (supplied by the MCA and the PCA, respectively) adjust the cerebral blood flow to changes in CO_2 concentration in different manners. However, no regional differences in cerebrovascular reactivity were reported [38]. The τ_{PFF} estimated from different cerebral arteries may then be used as an additional descriptor of regional cerebral hemodynamics during CO_2 challenges. However, further research is needed to test whether differences in the τ_{PFF} between cerebral arteries may provide additional evidence of differential anterior and posterior cerebrovascular reactivity.

Furthermore, it was shown that aging alters hemodynamic characteristics such as C_a and CVR, influencing cerebral circulation [39, 40]. Hence, the τ_{PFF}, that represents mutual independence between resistance and compliance, can be used to illustrate the differences in the mechanoelastic properties of the cerebral arteries in elderly people. In addition, the τ_{PFF} may provide information about how pathological processes related to vascular remodeling (e.g. ischemic stroke [41] or obesity [42]) change cerebral hemodynamic parameters in the different cerebral arteries.

Finally, our previous studies have shown that the τ, estimated using the CFF model, may provide valuable information for clinical practice. We demonstrated that the τ_{CFF} efficiently assesses cerebral hemodynamics in aneurysmal subanachroid hemorrhage (aSAH) patients [12]. Furthermore, we reported that a decrease in the τ_{CFF} can be observed earlier than the traditional characteristics of vasospasm, thus it can serve as an early-warning indicator of vessel narrowing [12]. The τ_{CFF} was also found as clinically relevant in patients with internal carotid artery (ICA) stenosis [13]. The τ_{CFF} estimated from the MCA was significantly shorter in patients with stenosis than in normal data. The τ_{CFF} was also found shorter in patients with traumatic brain injury (TBI) than in normal subjects, and significantly shorter in TBI patients with internal hematoma (IH) than in TBI patients without IH [43]. The results of other research performed in normal pressure hydrocephalus patients shown that although the τ_{CFF} is not linked to cerebrospinal fluid circulation, it is

correlated with CPP changes during an infusion test [44]. However, the interpretation of τ_{CFF} differs significantly from the interpretation of τ_{PFF}. Further studies will help to establish whether the τ estimated with PFF model may be also useful in the above-described clinical scenarios.

4.1 Limitations

The main limitation of this study is its model-based approach, with no confirmation via imaging methods (MRI or PET). We are aware that the results of the τ_{CFF} and τ_{PFF} calculated from the PCA and from the MCA need to be validated using MRI with mean transit time (MTT) and arterial arrival time (AAT). Moreover, the cerebral arterial pulse waveforms were estimated using arterial pressure pulses measured from the finger. The peripheral pressure may poorly reflect the cerebral pressure [45]; this is a methodological compromise, resulting from the non-invasive character of signal recording in healthy volunteers.

Due to the unknown cross-sectional area (S_a) of the insonated vessel, the value of the ΔC_aBV (both CFF and PFF) was normalized (divide by the S_a). This implies that the parameters including $Amp\Delta C_aBV$ cannot be compared between subjects (only relative changes are possible to assess). However, the τ_{CFF} and τ_{PFF} can be compared between volunteers because the S_a is removed as the result of multiplication (see Eqs. 10–11).

Furthermore, the number of analysed volunteers was limited. However, the group was homogenous with respect to age and enough to demonstrate the significant differences in τ of the MCA and the PCA. This study was a pilot observation of the τ_{PFF} differences, when estimated from the PCA and from the MCA. Thus, further study in a larger group of healthy volunteers is needed to confirm our observation and to prove its potential clinical application.

5 Conclusion

We demonstrated the differences in the TCD-based, non-invasive cerebral arterial time constant (τ) estimated from the MCA and from the PCA. The results suggest that the τ calculated using the pulsatile flow forward model better reflects the cerebral vascular differences in the brain lobes than does the continuous flow forward model.

Funding This research was supported by the National Science Centre (Poland) under Grant No. UMO-2013/10/E/ST7/00117.

Compliance with ethical standards

Conflict of interest ICM+ Software is licensed by Cambridge Enterprise, Cambridge, UK, http://www.neurosurg.cam.ac.uk/icmplus/. Prof. Czosnyka has a financial interest in a fraction of the licensing fee for ICM+ software. The other authors declare that they have no conflict of interest.

Informed consent The protocol complied with the Declaration of Helsinki of the World Medical Association, and all participants gave written informed consent before participating in the study. All patients had a study identification number and the data was anonymized before analysis.

Research involving human and animal rights This study was approved by the bioethical committee of the Wroclaw Medical University (permission no. KB—170/2014).

References

1. Ito H, Kanno I, Fukuda H. Human cerebral circulation: positron emission tomography studies. Ann Nucl Med. 2005;19:65–74. https://doi.org/10.1007/BF03027383.
2. Bhogal AA, Philippens MEP, Siero JCW, et al. Examining the regional and cerebral depth-dependent BOLD cerebrovascular reactivity response at 7T. Neuroimage 2015;114:239–48. https://doi.org/10.1016/j.neuroimage.2015.04.014.
3. Ito H, Kanno I, Takahashi K, et al. Regional distribution of human cerebral vascular mean transit time measured by positron emission tomography. Neuroimage 2003;19:1163–9. https://doi.org/10.1016/S1053-8119(03)00156-3.
4. Chen Y, Wang DJJ, Detre JA. Comparison of arterial transit times estimated using arterial spin labeling. MAGMA 2012;25:135–44. https://doi.org/10.1007/s10334-011-0276-5.
5. Haller S, Zaharchuk G, Thomas DL, et al. Arterial spin labeling perfusion of the brain: emerging clinical applications. Radiology 2016;281:337–56. https://doi.org/10.1148/radiol.2016150789.
6. Cardim D, Robba C, Bohdanowicz M, et al. Non-invasive monitoring of intracranial pressure using transcranial Doppler ultrasonography: is it possible? Neurocrit Care. 2016;25:473–91. https://doi.org/10.1007/s12028-016-0258-6.
7. Mascia L, Fedorko L, TerBrugge K, et al. The accuracy of transcranial Doppler to detect vasospasm in patients with aneurysmal subarachnoid hemorrhage. Intensive Care Med. 2003;29:1088–94. https://doi.org/10.1007/s00134-003-1780-5.
8. Kim D-J, Kasprowicz M, Carrera E, et al. The monitoring of relative changes in compartmental compliances of brain. Physiol Meas. 2009;30:647–59. https://doi.org/10.1088/0967-3334/30/7/009.
9. Uryga A, Kasprowicz M, Calviello L, et al. Assessment of cerebral hemodynamic parameters using pulsatile versus non-pulsatile cerebral blood outflow models. J Clin Monit Comput doi. 2018. https://doi.org/10.1007/s10877-018-0136-1.
10. Avezaat CJJ, van Eijndhoven JHM. The role of the pulsatile pressure variations in intracranial pressure monitoring. Neurosurg Rev. 1986;9:113–20. https://doi.org/10.1007/BF01743061.
11. Kasprowicz M, Diedler J, Reinhard M, et al. Time constant of the cerebral arterial bed in normal subjects. Ultrasound Med Biol. 2012;38:1129–37. https://doi.org/10.1016/j.ultrasmedbio.2012.02.014.
12. Kasprowicz M, Czosnyka M, Soehle M, et al. Vasospasm shortens cerebral arterial time constant. Neurocrit Care. 2012;16:213–8. https://doi.org/10.1007/s12028-011-9653-1.
13. Kasprowicz M, Diedler J, Reinhard M, et al. Time constant of the cerebral arterial bed. Acta Neurochir Suppl. 2012;114:17–21. https://doi.org/10.1007/978-3-7091-0956-4-4.
14. Czosnyka M, Richards HK, Reinhard M, et al. Cerebrovascular time constant: dependence on cerebral perfusion pressure and

end-tidal carbon dioxide concentration. Neurol Res. 2012;34:17–24. https://doi.org/10.1179/1743132811Y.0000000040.
15. van Eijndhoven JH, Avezaat CJ. Cerebrospinal fluid pulse pressure and the pulsatile variation in cerebral blood volume: an experimental study in dogs. Neurosurgery 1986;19:507–22.
16. Carrera E, Kim DJ, Castellani G, et al. Effect of hyper- and hypocapnia on cerebral arterial compliance in normal subjects. J Neuroimaging. 2011;21:121–5. https://doi.org/10.1111/j.1552-6569.2009.00439.x.
17. Uryga A, Placek MM, Wachel P, et al. Phase shift between respiratory oscillations in cerebral blood flow velocity and arterial blood pressure. Physiol Meas. 2017;38:310–24. https://doi.org/10.1088/1361-6579/38/2/310.
18. Aydin IH, Takçi E, Kadioğlu HH, et al. The variations of lenticulostriate arteries in the middle cerebral artery aneurysms. Acta Neurochir (Wien). 1996;138:555–9. https://doi.org/10.1007/BF01411176.
19. Kang CK, Park CA, Lee H, et al. Hypertension correlates with lenticulostriate arteries visualized by 7T magnetic resonance angiography. Hypertension 2009;54:1050–6. https://doi.org/10.1161/HYPERTENSIONAHA.109.140350.
20. Schmahmann JD. Vascular syndromes of the thalamus. Stroke 2003;34:2264–78. https://doi.org/10.1161/01.STR.0000087786.38997.9E.
21. Lazorthes G, Salamon G, Gouaze AZJ. The central arteries of the brain. Classification and territories of vascular supply. In: Salamon G, editor. Advances in cerebral angiography. Berlin: Springer; 1975. pp. 37–41.
22. Lin C-M, Tseng Y-C, Hsu H-L, et al. Arterial spin labeling perfusion study in the patients with subacute mild traumatic brain injury. PLoS ONE. 2016;11:e0149109. https://doi.org/10.1371/journal.pone.0149109.
23. Eames PJ, Potter JF, Panerai RB. Influence of controlled breathing patterns on cerebrovascular autoregulation and cardiac baroreceptor sensitivity. Clin Sci (Lond). 2004;106:155–62. https://doi.org/10.1042/CS20030194.
24. Sperna Weiland NH, Hermanides J, Hollmann MW, et al. Novel method for intraoperative assessment of cerebral autoregulation by paced breathing. Br J Anaesth. 2017;119:1141–49. https://doi.org/10.1093/bja/aex333.
25. Poyhonen M, Syvaoja S, Hartikainen J, et al. The effect of carbon dioxide, respiratory rate and tidal volume on human heart rate variability. Acta Anaesthesiol Scand. 2004;48:93–101. https://doi.org/10.1080/13548500903322791.
26. Battisti-Charbonney A, Fisher J, Duffin J. The cerebrovascular response to carbon dioxide in humans. J Physiol. 2011;589:3039–48. https://doi.org/10.1113/jphysiol.2011.206052.
27. Zamir M, Moir ME, Klassen SA, et al. Cerebrovascular compliance within the rigid confines of the skull. Front Physiol. 2018;9:940. https://doi.org/10.3389/fphys.2018.00940.
28. Donnelly J, Budohoski KP, Smielewski P, Czosnyka M. Regulation of the cerebral circulation: bedside assessment and clinical implications. Crit Care. 2016;20:129. https://doi.org/10.1186/s13054-016-1293-6.
29. Kim D-J, Czosnyka Z, Kasprowicz M, et al. Continuous monitoring of the Monro-Kellie doctrine: is it possible? J Neurotrauma. 2012;29:1354–63. https://doi.org/10.1089/neu.2011.2018.
30. Zamir M. The physics of coronary blood flow. 1st ed. Boston: Springer; 2005.
31. Kasprowicz M, Czosnyka M, Poplawska K, Reinhard M. Cerebral arterial time constant recorded from the MCA and PICA in normal subjects. Acta Neurochir Suppl. 2016;122:211–4. https://doi.org/10.1007/978-3-319-22533-3_42.
32. Tayebi Meybodi A, Lawton MT, Feng X, Benet A. Posterior inferior cerebellar artery reimplantation: buffer lengths, perforator anatomy, and technical limitations. J Neurosurg. 2016;125:909–14. https://doi.org/10.3171/2015.8.JNS151411.
33. Párraga RG, Ribas GC, Andrade SEGL, De Oliveira E. Microsurgical anatomy of the posterior cerebral artery in three-dimensional images. World Neurosurg. 2011;75:233–57. https://doi.org/10.1016/j.wneu.2010.10.053.
34. MacIntosh BJ, Filippini N, Chappell MA, et al. Assessment of arterial arrival times derived from multiple inversion time pulsed arterial spin labeling MRI. Magn Reson Med. 2010;63:641–7. https://doi.org/10.1002/mrm.22256.
35. Skow RJ, MacKay CM, Tymko MM, et al. Differential cerebrovascular CO_2 reactivity in anterior and posterior cerebral circulations. Respir Physiol Neurobiol. 2013;189:76–86. https://doi.org/10.1016/j.resp.2013.05.036.
36. Willie CK, Macleod DB, Shaw AD, et al. Regional brain blood flow in man during acute changes in arterial blood gases. J Physiol. 2012;590:3261–75. https://doi.org/10.1113/jphysiol.2012.228551.
37. Sato K, Sadamoto T, Hirasawa A, et al. Differential blood flow responses to CO_2 in human internal and external carotid and vertebral arteries. J Physiol. 2012;590:3277–90. https://doi.org/10.1113/jphysiol.2012.230425.
38. Hida W, Kikuchi Y, Okabe S, et al. CO_2 response for the brain stem artery blood flow velocity in man. Respir Physiol. 1996;104:71–5. https://doi.org/10.1016/0034-5687(96)00011-4.
39. Yang D, Cabral D, Gaspard EN, et al. Cerebral hemodynamics in the elderly: a transcranial doppler study in the Einstein aging study cohort. J Ultrasound Med. 2016;35:1907–14. https://doi.org/10.7863/ultra.15.10040.
40. Robertson AD, Tessmer CF, Hughson RL. Association between arterial stiffness and cerebrovascular resistance in the elderly. J Hum Hypertens. 2010;24:190–6. https://doi.org/10.1038/jhh.2009.56.
41. Liu J, Wang Y, Akamatsu Y, et al. Vascular remodeling after ischemic stroke: mechanisms and therapeutic potentials. Prog Neurobiol. 2014;115:138–56. https://doi.org/10.1016/j.pneurobio.2013.11.004.
42. Osmond JM, Mintz JD, Dalton B, Stepp DW. Obesity increases blood pressure, cerebral vascular remodeling, and severity of stroke in the Zucker rat. Hypertension 2009;53:381–6. https://doi.org/10.1161/HYPERTENSIONAHA.108.124149.
43. Trofimov A, Kalentiev G, Gribkov A, et al. Cerebrovascular time constant in patients with head injury. Acta Neurochir Suppl. 2016;121:295–7. https://doi.org/10.1007/978-3-319-18497-5_51.
44. Capel C, Kasprowicz M, Czosnyka M, et al. Cerebrovascular time constant in patients suffering from hydrocephalus. Neurol Res. 2014;36:255–61. https://doi.org/10.1179/1743132813Y.0000000282.
45. Panerai RB, Sammons EL, Smith SM, et al. Transient drifts between Finapres and continuous intra-aortic measurements of blood pressure. Blood Press Monit. 2007;12:369–76. https://doi.org/10.1097/MBP.0b013e3282c9ad2f.